ACS APPLIED MATERIALS & INTERFACES

www.acsami.org

Research Article

Proton Logic Gate Based on a Gramicidin-ATP Synthase Integrated Biotransducer

Yukun Chen, Gábor Méhes, Bingfu Liu, Liyun Gao, Mingyin Cui, Chenliang Lin, Yoko Hirono-Hara, Kiyotaka Y. Hara, Noriyo Mitome, and Takeo Miyake*

Cite This: *ACS Appl. Mater. Interfaces* 2024, 16, 7480–7488

Read Online

ACCESS | Metrics & More | Article Recommendations | Supporting Information

ABSTRACT: Ion channels are membrane proteins that allow ionic signals to pass through channel pores for biofunctional modulations. However, biodevices that integrate bidirectional biological signal transmission between a device and biological converter through supported lipid bilayers (SLBs) while simultaneously controlling the process are lacking. Therefore, in this study, we aimed to develop a hybrid biotransducer composed of ATP synthase and proton channel gramicidin A (gA), controlled by a sulfonated polyaniline (SPA) conducting polymer layer deposited on a microelectrode, and to simulate a model circuit for this system. We controlled proton transport across the gA channel using both electrical and chemical input signals by applying voltage to the SPA or introducing calcium ions (inhibitor) and ethylenediaminetetraacetic acid molecules (inhibitor remover). The insertion of gA and ATP synthase into SLBs on microelectrodes resulted in an integrated biotransducer, in which the proton current was controlled by the flux of adenosine diphosphate molecules and calcium ions. Lastly, we created an XOR logic gate as an enzymatic logic system where the output proton current was controlled by Input A (ATP synthase) and Input B (calcium ions), making use of the unidirectional and bidirectional transmission of protons in ATP synthase and gA, respectively. We combined gA, ATP synthase, and SPA as a hybrid bioiontronics system to control bidirectional or unidirectional ion transport across SLBs in biotransducers. Thus, our findings are potentially relevant for a range of advanced biological and medical applications.

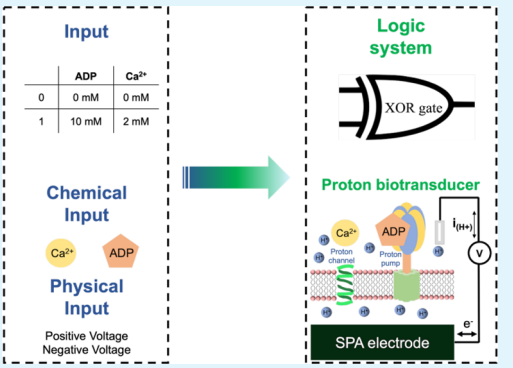

KEYWORDS: *biotransducer, logic gate, ATP synthase, gramicidin A, supported lipid bilayers*

1. INTRODUCTION

Microfabricated bioelectrical devices (biodevices) play an important role in medical and other biological research by interconverting biological and electrical signals. For example, miniature biofuel cells have recently been used as wearable devices for extracting power from glucose[1] and biological fluids,[2] including human sweat,[3] and for powering smart contact lenses.[4] Organic mixed ionic-electronic conductors, such as conducting polymers, have been successfully used to bridge the gap between biological and electrical systems.[5,6] Another biodevice, bioelectrical delivery device, has been used to release molecules from storage materials, such as insulin from hydrogels,[7,8] acetylcholine from PVC selective electrodes,[9] and protons from palladium hydride.[10] Ions and molecules, information carriers in biological communications and energy currencies in biodevices,[11] have been the subject of many recent studies, mainly focusing on modulation and sensing via biotransducers,[12] transistors,[13] and electrophoretic delivery devices.[14] To study ion transport, most researchers use biotransducers that employ various ion transport channels and supported lipid bilayers (SLBs) as transport pathways and carriers, respectively. In particular, DNA nanopores,[15] ion channels,[16] ATP synthases,[17] and carbon nanotubes[18] serve as pathways across SLBs in transporting ions and molecules. Molecular transport across SLBs have been demonstrated using proteins on various platforms, including silicon nanowires[19,20] and carbon nanotubes.[21] However, devices that can integrate bidirectional biological signal transmission between a device and biological converter through SLBs while simultaneously controlling the process are lacking. Realizing such a system would enable the modulation of biological functions at the cellular level, which is important for fundamental studies and advanced bioengineering. We integrated an ATP synthase-based biosystem on a microelectrode decorated with sulfonated polyaniline (SPA) to control proton flow across an ATP synthase, which in turn modulated an enzyme cascade reaction, fueling luciferase-luciferin bioluminescence.[22] This modulation was achieved by the excellent proton and ion selectivities, owing to the electron−proton coupling of the

Received: October 12, 2023
Revised: January 10, 2024
Accepted: January 15, 2024
Published: January 31, 2024

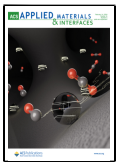

https://doi.org/10.1021/acsami.3c15251
ACS Appl. Mater. Interfaces 2024, 16, 7480−7488

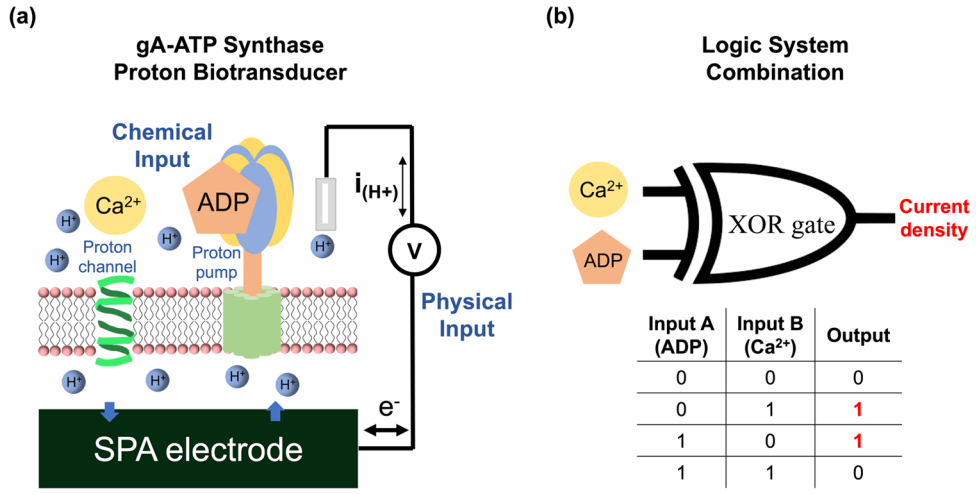

Figure 1. Description of proton logic gate hybrid device. (a) Principle of hybrid biotransducer system interfacing a sulfonated polyaniline (SPA) electrode with gramicidin A (gA) and ATP synthase. Chemical inputs are Ca^{2+} and ADP, and the physical input is voltage. SPA releases/absorbs protons below the membrane, and the resulting protonic gradient (ΔpH) across the membrane drives proton transport through it. Ca^{2+} and ADP control the proton transport across the gA ion channel and ATP synthase, respectively, and the controllable current is measured as the output signal. (b) Integrated gA-ATP synthase biotransducer with the XOR logic system and the corresponding truth table.

SPA-conducting polymer-based electrode. To expand the versatility of this biodevice, we aimed to achieve and control the bidirectional transport of protons across SLBs. In particular, biotransducers can be applied in enzyme logic gates which enable the manipulation and processing of signals and data and have potential applications in biotechnology and medicine for tasks such as signal readout and sensor concepts.[23] However, studies on logic gates utilizing enzyme-catalyzed biochemical reactions combined with transducers,[24−26] showing promising potential for future development and implementation in biochemical computing systems are few. Therefore, in this study, we aimed to develop a hybrid proton transport system that integrates the unidirectional transport of protons across SLBs via ATP synthase and bidirectional transport via the proton channel gramicidin A (gA; Figure 1a). We inserted gA into SLBs deposited onto SPA-decorated gold microelectrodes to serve as a capacitive element in the electrode structure. To gain insight into this bioelectrical system, we developed an equivalent electrical circuit model and verified it using electrochemical impedance spectroscopy (EIS). We successfully controlled the transport of protons across gA ion channels by adding Ca^{2+} and ethylenediaminetetraacetic acid (EDTA). We then integrated both gA and ATP synthase to confer control over both the bidirectional and unidirectional transport of proton currents across the SLBs. Finally, this hybrid system was used to demonstrate a biological logic gate, where, for the first time, a measurable electrical output was activated by two chemical inputs and one voltage input. More concretely, the proton currents across the SLBs were the output signals of the logic gate; Ca^{2+} and ADP were the two chemical inputs, and the applied voltage was the physical input signal to control the output. By controlling proton transport in gA and ATP synthase, we developed a proton biotransducer XOR logic gate (Figure 1b). We successfully demonstrated the control of the H^+ current in both bidirectional and unidirectional transport modes using this hybrid system.

2. EXPERIMENTAL SECTION

2.1. Materials. Acetonitrile (anhydrous, 99.8% purity), aniline (≥99.5% purity), and fluorosulfonic acid (HSO_3F) were purchased from Sigma-Aldrich. Gramicidin A (antibiotic agent) was purchased from Abcam, alamethicin (≥98% purity, *Trichoderma viride*) from Sigma-Aldrich, and 1,2-dioleoyl-*sn*-glycero-3-phosphocholine (DOPC, >97.0% purity) from Tokyo Chemical Industry Co. K_2HPO_4, HCl, KH_2PO_4, KCl, NaOH, and $CHCl_3$ were purchased from Wako. The substrates were 2 in. diameter silicon wafers (Shunsheng Electronics Co., China). The K-PBS buffer solution was prepared using deionized water (EYELA), 100 mM KCl, 3 mM K_2HPO_4, and 2 mM KH_2PO_4 and adjusted to pH 7.0, while monitoring with a pH meter (Horiba Scientific, Japan).

2.2. Au Microelectrode Fabrication and SPA Polymerization. The biotransducer is the same as that in our previous study.[22] The microelectrode fabrication process is shown in Supporting Figure S1. The S1818 photoresist was spin-coated on a cleaned and oxidized 50 nm thick silicon wafer, a specific pattern was obtained by photolithographic development, and gold was deposited by vacuum evaporation. Excess gold was removed using a Remover PG (Kayaku Advanced Materials, Inc.) to obtain gold electrodes. Finally, an insulating SU-8 photoresist was spin-coated onto the electrode, and the excess part was removed by photolithography to obtain the microelectrode. The microfluidic channel was made from polydimethylsiloxane (PDMS). For EIS measurements, we used gridded Au microelectrodes with an area of 100 × 200 μm^2 to reduce measurement noise. In the case of the current measurement, the areas of the Au microelectrodes were 7 × 10, 7 × 20, 7 × 30, 7 × 40, and 7 × 50 μm^2. The PDMS containers were made and mounted on an Au-patterned Si wafer. SPA films were polymerized using 100 mM aniline and 200 mM HSO_3F in an acetonitrile solution onto an Au microelectrode surface by using an HSV-110 three-electrode system (Hokuto Denko, Japan), applying 15 cycles of cyclic voltammograms [ranging from −0.30 to +1.90 V (vs Ag/AgCl) at a sweep rate of 100 mV s^{-1}]. After the electropolymerization, the SPA-coated electrodes were washed with deionized water. To set the initial pH, the SPA biotransducer was immersed in a K-PBS buffer solution.

2.3. SLB Formation and Ion Channel Incorporation. We dissolved the DOPC powder in chloroform, evaporated it with N_2 gas, and redissolved it in K-PBS solution (pH 7) to yield 0.5 mg mL^{-1} DOPC solution. The prepared DOPC solution was sonicated, and the vesicles were collected using a 100 nm diameter filter. To form the SLBs on the SPA electrode, the vesicle solution was dropped into the microfluidic channel and gently shaken for 12 h at 100% humidity.

https://doi.org/10.1021/acsami.3c15251
ACS Appl. Mater. Interfaces 2024, 16, 7480−7488

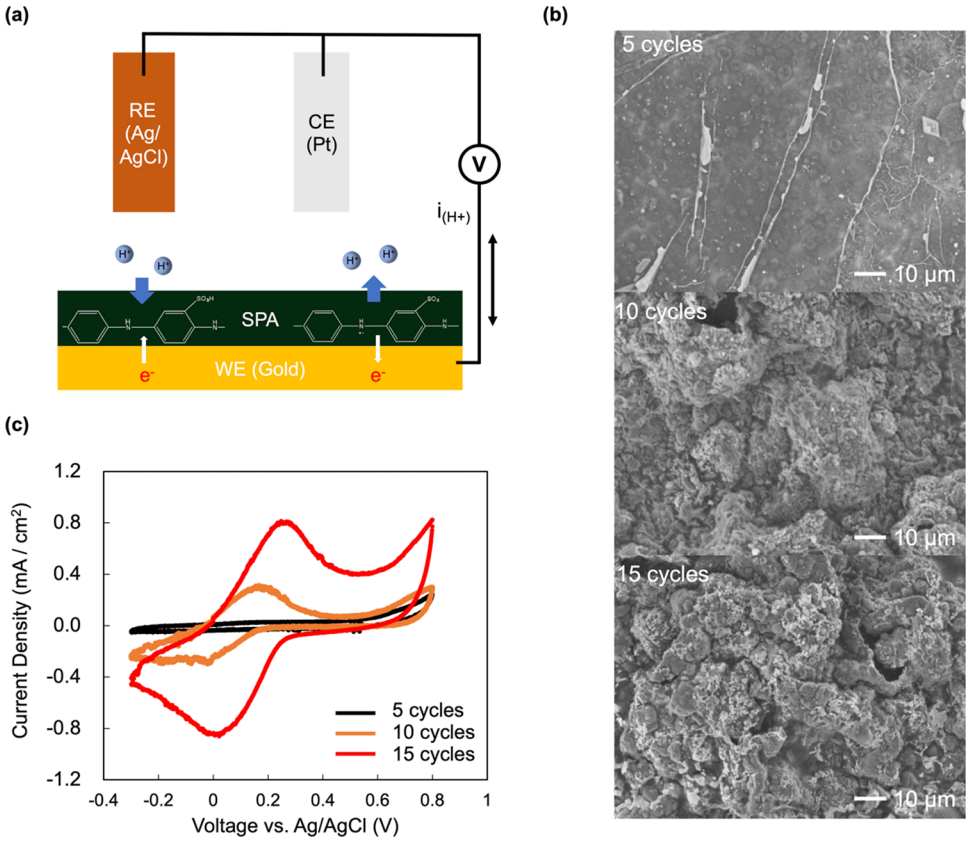

Figure 2. Structure and performance of sulfonated polyaniline (SPA) biotransducer. (a) SPA biotransducer fabrication by electropolymerization with three-electrode system (WE: working electrode, CE: counter electrode, RE: reference electrode), and biotransducer property measurements in K-PBS solution. (b) SEM images taken after electropolymerization of SPA using 5, 10, and 15 cycles of cyclic voltammetry (CVs). (c) Representative CV curves taken during electropolymerization of SPA onto gold microelectrode in K-PBS buffer solution with different cycle numbers.

After SLB formation, gA dissolved in 99% ethanol was added to a 150 μL microfluidic chamber to integrate the gA into the SLBs. For the current measurement, gA dissolved in 99% ethanol was mixed with DOPC dissolved in chloroform, followed by evaporation of the solvent with N_2 and the addition of a K-PBS buffer solution. In the gA-only control experiment, the concentrations of gA and ATP synthase were 3 and 0.6 μmol L^{-1}, respectively. This solution was sonicated to obtain a small-molecule DOPC solution containing gA. The solution was then added to the microfluidic chamber to obtain SLBs doped with gAs. For the insertion of alamethicin (ALM), after the SLBs were covered, the K-PBS solution, in which ALM was dissolved, was directly added to the device to obtain SLBs doped with ALM.

2.4. ATP Synthase Preparation. We used the same ATP synthase (F_oF_1 ATP synthase from thermophilic *Bacillus* PS3) as that in our previous paper. All of the preparation and detection procedures were as described previously.[22]

2.5. ATP Synthase Integration. To integrate the ATP synthase into the SLBs, 30 μL of 5 mg mL^{-1} ATP synthase solution was added to a 150 μL microfluidic chamber after the SLB formation.

2.6. Electrical Measurement. For the EIS measurements, we connected the SPA and Ag/AgCl (KCl) electrodes as the working and counter electrodes, respectively, to an electrochemical analyzer (ALS Model 704E, BAS, Japan). We applied a 10 mV AC voltage with no DC bias from 100 MHz to 0.1 Hz. For current measurements in gA, we connected the SPA working electrode and Ag/AgCl reference electrode to a semiconductor device analyzer (B1500A, Keysight). For the measurements, we applied voltages to the device in the presence and absence of 1 mM Ca^{2+} and 2 mM ADP and then measured the current for 1 min.

3. RESULTS AND DISCUSSION

3.1. Optimization and Operation of SPA-Based H^+ Biotransducer. An SPA layer coated onto a gold microelectrode via electropolymerization by cyclic voltammetry (CV) served as a proton biotransducer. H^+ ions were transferred between the SPA layer and the solution by applying appropriate potentials to the SPA electrode versus an Ag/AgCl reference electrode (Figure 2a).[27] Typically, the number of CV cycles applied during electropolymerization can substantially affect the structure and properties of the prepared polymeric layers.[28,29] To investigate these effects and optimize our electrode, we compared the charge transfer kinetics in a three-electrode system (Figure 2a) and the surface morphology captured by scanning electron microscopy (SEM, Figure 2b) of different layers of SPA fabricated by 5, 10, and 15 CV cycles (Figure 2c). The SEM images revealed distinct patterns when differently prepared SPA layers were compared. At 5 CV cycles, minimal polymerization was observed, and at 10 cycles, SPA started to polymerize on the electrode surface, exhibiting its characteristic structure. At 15 CV cycles, a greater amount of SPA was deposited with a more pronounced surface structure. Increasing the number of CV cycles resulted in a prominent polymerization of SPA on the electrode surface, indicating that optimizing the parameters of electrochemical deposition plays a crucial role in increasing the amount and surface roughness of SPA on the electrode, which is expected to lead to an enhanced biotransduction in the final device. In accordance with the SEM observations, with the increase of

https://doi.org/10.1021/acsami.3c15251
ACS Appl. Mater. Interfaces 2024, 16, 7480−7488

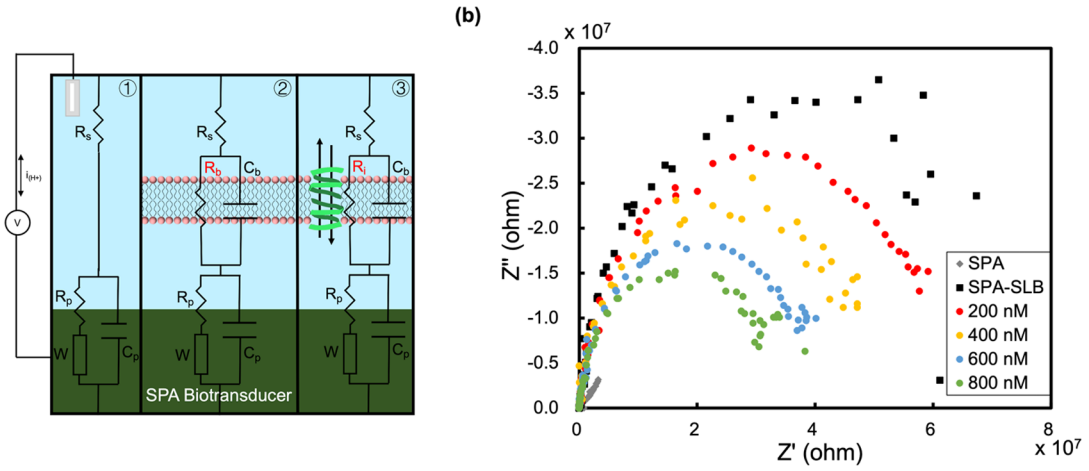

Figure 3. Model structure and AC impedance data of supported lipid bilayer (SLB) biotransducer. (a) Equivalent circuit model and structure of the gA-SLB-device. (b) Electrochemical impedance spectroscopy measurement of the SLB deposited electrode at different concentrations of gramicidin A (gA). The drawing in (a) shows the presence of gA-SLBs. SPA, sulfonated polyaniline.

cycle numbers, we observed larger oxidation and reduction currents in the voltage ranges from 0 to +0.4 V and from −0.3 to +0.2 V (Figure 2a; all voltages were in reference to Ag/AgCl), corresponding to the number of protons released and absorbed by the SPA layer, respectively. We utilized SPA microelectrodes to control the absorption and release of protons by applying a voltage with the aim to create a proton concentration gradient at the interface between the microelectrode and SLB. This gradient, known as proton motive force (PMF), is a fundamental mechanism observed in a wide range of biological systems. PMF (Δp) provides the necessary energy for driving proton transport through ion pumps,[30] and is defined as

$$\Delta p = \Delta\mathrm{pH} + \Delta\psi \quad (1)$$

where $\Delta\mathrm{pH} = \mathrm{pH}_{(\mathrm{in})} - \mathrm{pH}_{(\mathrm{out})}$ and $\Delta\psi = E_{(\mathrm{in})} - E_{(\mathrm{out})}$ are the pH gradient and the potential difference between the inside and outside of SLB, respectively. The application of a positive/negative voltage cycle to the SPA electrode to inject/absorb H^+ ions into/from the nanolayer between the SPA and SLBs resulted in an increase/decrease in both the ΔpH and $\Delta\psi$. In addition to the proton gradient, the applied voltage also affected (increase/decrease) $\Delta\psi$. When the positive or negative Δp reached a certain value, ions started to transport out of or into the membrane. The application of voltage to control PMF created a pH gradient that transported protons across both gA and ATP synthase in bidirectional and unidirectional ways, respectively.

3.2. Equivalent Circuit Model of gA/SPA Biotransducers. To investigate the SLB formation and confirm the biotransduction process after the introduction of gA into the SPA biotransducer, we determined the resistive and capacitive properties of the device by using EIS measurements. We observed that when the SLB binds to the electrode, the equivalent circuit model requires the addition of new high-impedance elements to fit the measured data. When an ion channel or a protein binds to the SLBs and penetrates the SLBs for transporting ions, the element representing the impedance of SLBs decreases.[31,32] We conducted a comparative analysis of EIS data from different groups of samples, including SPA only, SPA with deposited SLBs, and SLBs with varying concentrations of gA. Figure 3a shows a circuit model for analyzing the measured data. When only SPA was polymerized on the Au electrode (case 1 in Figure 3a), the circuit was considered to have polymer resistance (R_p), in parallel with polymer capacitance (C_p), and Warburg diffusion element (W)[33] and in series with electrolyte resistance (R_s). When the SLBs were deposited on the SPA (case 2 in Figure 3a), two new elements were added to the circuit: SLB resistance (R_b) and capacitance (C_b), which were connected in parallel with each other and in series with the SPA circuit. Finally, the integration of gA into the SLBs (case 3 in Figure 3a) was modeled by exchanging R_b with gA and SLB resistance (R_i). This suggests that the insertion of gA does not change the number of circuit elements; it changes only the SLB properties. The comparison of the Nyquist plots of cases 1−3 showed the transition from a straight line to a large semicircle when SLBs were formed on the SPA electrode, indicating a change from a diffusion-limited mode to weak charge transfer at low frequencies. However, with an increase in the concentration of gA, we observed a decrease in the size of the semicircles, indicating the successful integration of gA into the SLBs and the transition from R_b to R_i, while simultaneously decreasing R_i (Figure 3b), as listed in Table 1. The fitted lines based on the equivalent circuit model described above are shown in Supporting Figure S2, and the extracted fitting parameters are listed in Supporting Information, Table S1. Preliminarily, we assumed that such a decreasing trend in R_b indicates an increase in proton transport through gA.

Table 1. Supported Lipid Bilayer (SLB) Resistance (R_b; only DOPC) and Gramicidin (gA) and SLB Resistance (R_i; Different Concentrations of gA in DOPC) in H^+-Biotransducer

R_b (only DOPC) and R_i (different mol gA in DOPC)				
R_b (0 nM)	R_i (200 nM)	R_i (400 nM)	R_i (600 nM)	R_i (800 nM)
61.4 MΩ	54.1 MΩ	42.1 MΩ	34.5 MΩ	29.5 MΩ

Before gA was added, the value of R_p was 61.4 MΩ. After addition of gA into the device, gA integrated into SLBs and proton transport occurred in the gA ion channel. Consequently, we assumed that R_p changes to R_i, and the value of the resistance decreases, and at every 200 nM of gA added, R_i decreases approximately by 8 MΩ. This behavior was

https://doi.org/10.1021/acsami.3c15251
ACS Appl. Mater. Interfaces 2024, 16, 7480−7488

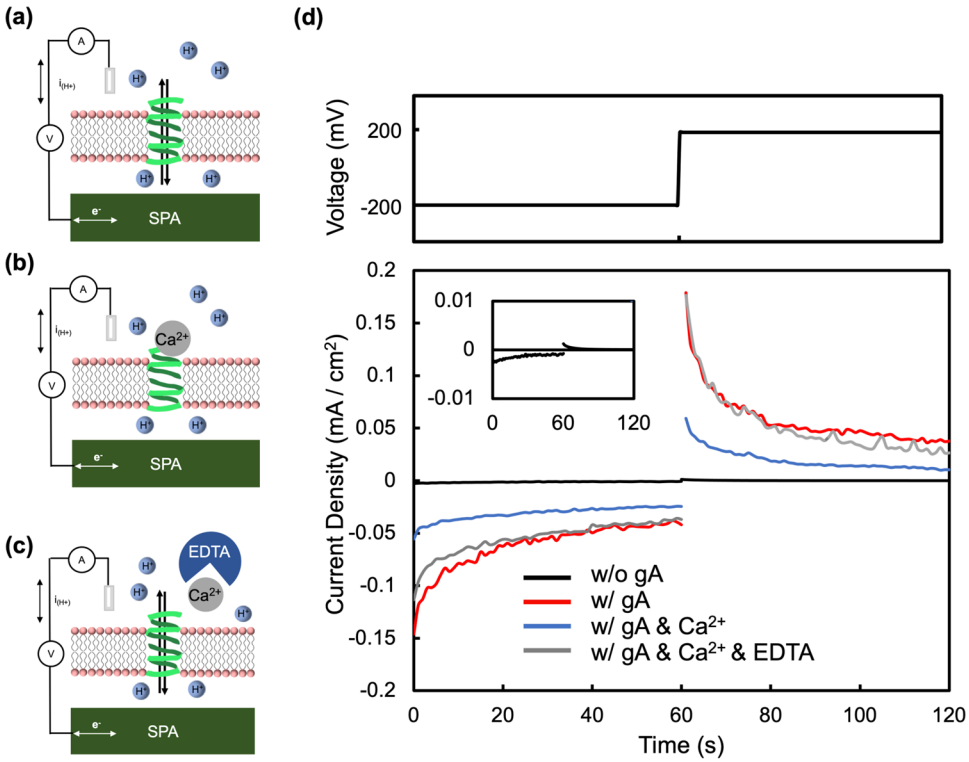

Figure 4. Control of proton current through gramicidin A (gA) in biotransducer. (a) Schematic diagram of the biotransducer integrated with gA, and measurement principle of the current at ±200 mV applied between the sulfonated polyaniline (SPA) and Ag/AgCl electrodes. (b) Measurement principle of the current signal at ±200 mV in buffer solution in the presence of 1 mM Ca^{2+}. (c) Measurement principle of the current signal at ±200 mV in buffer solution in the presence of 1 mM Ca^{2+} and 10 mM EDTA. (d) *I*–*t* curves corresponding to (a–c). Red, blue, and gray lines correspond to (a–c), respectively. The black line represents SLB-SPA biotransducer without gA. The inset is a zoom-in on the data set without gA ("w/o gA", black line). "w/gA" means with gA.

confirmed by the insertion of gA into the SLBs, which enabled ion transport between the membranes, thereby reducing the SLB impedance. In conclusion, EIS measurements showed that a new resistance element was added to the SPA biotransducer upon SLB deposition, indicating successful SLB coating on the SPA electrode. Moreover, the incorporation of gA decreased the real part of the impedance (resistance), demonstrating that gA can create proton transport capabilities through the SPA/SLB biotransducer.

3.3. Proton Control in gA. We utilized an SPA biotransducer to measure and control ion transport through the gA channel. Gramicidin A has been widely used in various SLB-based devices because of its ability to form transmembrane ion channels in SLBs, enabling the passage of cations. To demonstrate the use of an SPA biotransducer to control proton transport through gA, we applied voltage to an SPA electrode with integrated gA-SLBs and measured the response current vs Ag/AgCl in a two-electrode system, where the reference electrode was shorted to the counter electrode (Figure 4a). To assert control over proton transport through gA, we used calcium ions as inhibitors to block gA (Figure 4b) because Ca^{2+} is relatively large and thus blocks the gA ion channel.[34] To open the gA channel for proton flow, we removed Ca^{2+} ions using EDTA, which efficiently binds to this ion[35] (Figure 4c). Figure 4d displays the current densities when −200 mV was applied to the SPA electrode, followed by a step potential of +200 mV when gA, Ca^{2+}, and EDTA were gradually added to the buffer solution. Current signal was not observed at ±200 mV in the absence of gA (black line), indicating that protons cannot flow through lipid bilayers; therefore, SLBs show a good insulation property. We observed a relatively large signal (0.035 mA cm^{-2}, 3.52 mC cm^{-2}) at ±200 mV in the presence of gA (red line), and a 3 times smaller signal (0.011 mA cm^{-2}, 1.18 mC cm^{-2}) with the addition of Ca^{2+} inhibitor (blue line). The addition of EDTA resulted in the recovery of current signal, reaching values close to those recorded before EDTA addition (0.029 mA cm^{-2}, 3.17 mC cm^{-2}; gray line). The slightly lower signal after the addition of EDTA compared to only gA in the solution could be explained by some of the gA channels being blocked by the EDTA-chelating agent. We also confirmed that EDTA will not affect gA in the absence of Ca^{2+} (Supporting Figure S3). Moreover, by further analyzing different samples (Supporting Figure S4) we came to the conclusion that the current corresponding to proton transport through the gA can be controlled by the SPA biotransducer in the presence of chemical inhibitors/enablers.

To further substantiate the ability of the biotransducer to control proton transport across SLBs, we replaced gA with ALM, an antibiotic peptide ion channel with voltage-gated channel characteristics (Supporting Figure S5). When we applied ±200 mV without ALM, no current flowed. When we applied ±200 mV, a proton current was recorded, indicating that the ALM voltage-gated ion channel is open. Thus, the flow of protons in ALM voltage-gated ion channels can be controlled via the biotransducer, potentially indicating the versatility of our device for the insertion and use of various ion channels. However, both gA and ALM facilitate the bidirectional transport of protons, which may limit some advanced iontronic applications that require unidirectional ion flow. To

https://doi.org/10.1021/acsami.3c15251
ACS Appl. Mater. Interfaces 2024, 16, 7480−7488

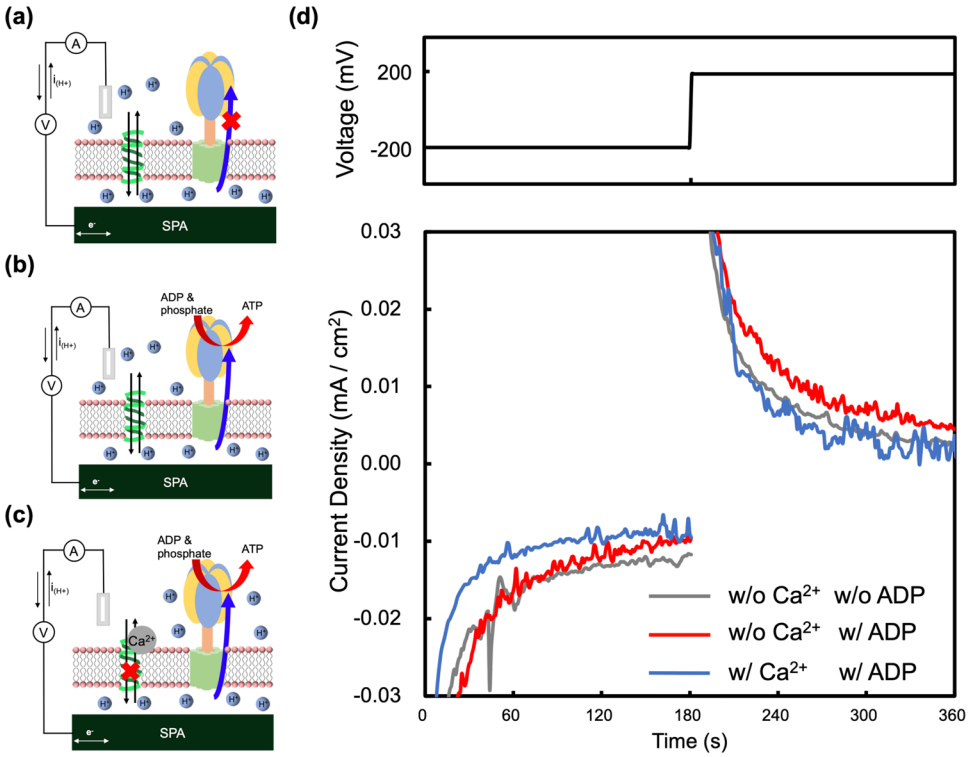

Figure 5. Control of gramicidin A (gA) and ATP synthase hybrid system integrated with the biotransducer. (a) Schematic representation of the gA and ATP synthase hybrid system integrated with the biotransducer and measurement principle of current at ±200 mV between the sulfonated polyaniline (SPA) and Ag/AgCl electrodes. (b) Measurement principle of the current signal at ±200 mV in buffer solution in the presence of 2 mM ADP. (c) Measurement of the current signal at ±200 mV in a buffer solution in the presence of 2 mM ADP and 1 mM Ca^{2+}. (d) *I*–*t* curves corresponding to (a–c). Gray, red, and blue lines correspond to (a–c), respectively.

control the proton transport between SLBs to a higher degree, it is important to design a system in which both bidirectional and unidirectional proton transport can be achieved and controlled.

3.4. Proton Control in a gA/ATP Synthase Hybrid System. We successfully controlled bidirectional proton transport across SLBs by applying a voltage to SPA proton biotransducers, thereby facilitating ATP hydrolysis and synthesis reactions in ATP synthase.[22] To further enhance control over the proton current in the biotransducer, we demonstrated a hybrid system that integrates the ion channel gA and the ion pump ATP synthase, enabling the modulation of proton transport in two distinct pathways. The hybrid system was regulated by inducing a proton current flow by using an externally applied voltage and added chemicals. To fabricate the hybrid system, we first deposited SLBs containing gA onto the SPA electrode and then introduced ATP synthase into the device. To control the proton transport through gA alone, we applied a voltage signal without adding any controlling chemicals (Figure 5a). In turn, the voltage-induced proton gradient induced transport of the proton through ion channels. To activate proton transport through ATP synthase, we introduced ADP molecules and simultaneously applied voltage to drive the ATP synthesis. This led to the simultaneous transport of protons by both ATP synthase and ion channel gA (Figure 5b). To exclusively control proton transport through ATP synthase, we used calcium ions as inhibitors to block gA function (Figure 5c). Figure 5d displays the current densities when −200 mV were applied to the SPA electrode, followed by a step potential of +200 mV when no chemicals were added and when ADP and Ca^{2+} were gradually added into the buffer solution. These potentials were chosen because the gA channel primarily mediated proton transport under either voltage polarity, whereas PMF drove proton transport through SLBs via ATP synthase only at +200 mV. The current signals observed at −200 mV in both the presence (red line) and absence (gray line) of ADP are relatively small, indicating that only the gA channel is responsible for transporting protons across the SLBs under these conditions. However, when +200 mV was applied, the current signal in the presence of ADP ($I_{(\text{gA and synthase current})}$ = 0.005 mA cm^{-2}, 2.64 mC cm^{-2}) was larger than that in the absence of ADP ($I_{(\text{gA current})}$ = 0.003 mA cm^{-2}, 2.08 mC cm^{-2}), indicating the involvement of both gA channel and ATP synthase in proton transport. A decrease in the current signal (blue line; $I_{(\text{synthase current})}$ = 0.002 mA cm^{-2}, 1.98 mC cm^{-2}), at −200 and +200 mV, when both Ca^{2+} and ADP were present confirmed that the initial current can primarily be attributed to the gA channel. To induce a current flow originating only from transport by ATP synthase, the gA channel was blocked by Ca^{2+}. Also, we saw the same behavior with the order of adding Ca^{2+} and ADP (Supporting Figure S6). When the three different currents at +200 mV were compared, the following relationship was observed:

$$I_{(\text{synthase current})} + I_{(\text{gA current})} \cong I_{(\text{gA \& synthase current})}$$

However, the Coulomb density calculation was not equivalent to that in the above equation. This discrepancy may be due to variations in proton absorption and release at the SPA electrode.[36] In contrast, the increase and decrease in the total charge when ADP and Ca^{2+} were added, respectively, indicate that the biotransducer modulates the gA-ATP synthase hybrid system through the application of voltage

https://doi.org/10.1021/acsami.3c15251
ACS Appl. Mater. Interfaces 2024, 16, 7480−7488

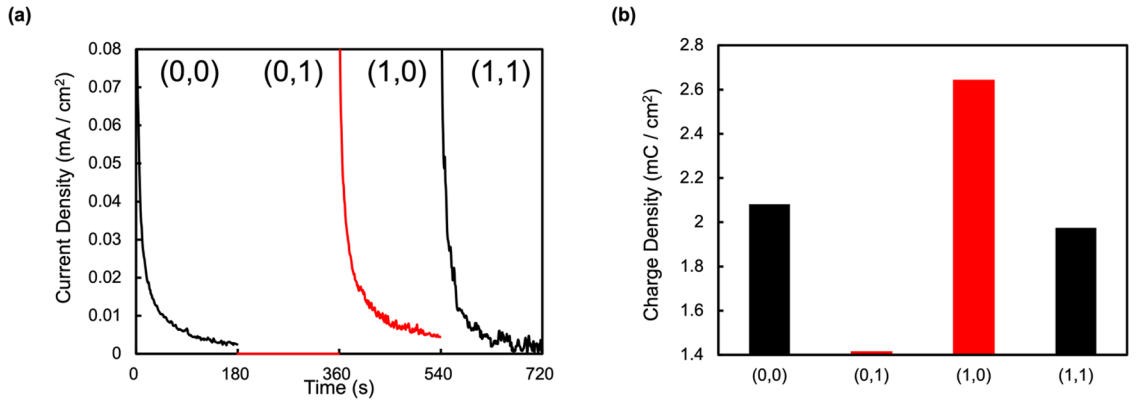

Figure 6. XOR logic gates combined with biotransducer. Input A and Input B are ADP and Ca^{2+}, respectively. (a) Current densities of 4 different input conditions, at V = +200 mV vs Ag/AgCl. (b) Charge densities of 4 different input conditions, at V = +200 mV vs Ag/AgCl.

and the introduction of two distinct chemical inputs. We confirmed this behavior for different samples, as shown in Supporting Figure S7. These findings demonstrate effective regulation of proton transport in the gA-ATP synthase hybrid system in SPA-SLBs and that either the gA channel or ATP synthase can be independently controlled by introducing the corresponding chemical input signal.

3.5. Hybrid Biotransducers Used as Different Logic Gates. Logic gates, which encompass ion channels, can be integrated with biological systems, making them suitable for constructing relatively complex logic circuits and allowing the utilization of ion and electron coupling signals for computation tasks. This can provide a biocompatible and efficient approach for future information processing. To investigate the integrability of our gA-ATP synthase hybrid system as a biotransducer in a biological system, we designed an experiment aimed at controlling and reading proton currents in the gA ion channel and ATP synthase using chemical inputs (Ca^{2+} and ADP) as control signals. Based on our investigations of proton transport control through gA and ATP synthase, we found that gA alone could not build a functional logic gate system, whereas ATP synthase could be integrated into an AND gate (Supporting Tables S2 and S3). Subsequently, we constructed an XOR logic system that can be achieved only by integrating both gA and ATP synthases with the SPA biotransducer. A key consideration for realizing such an XOR logic element is to utilize proton transport through the gA ion channel and ATP synthesis reaction while maintaining a positive voltage on both gA and ATP synthase. The XOR logic gate was constructed with two inputs: Ca^{2+} (0 mM ≅ 0 and 10 mM ≅ 1, where 0 = false and 1 = true in Boolean algebra) and ADP (0 mM ≅ 0 and 2 mM ≅ 1). We noted that this XOR logic behavior did not arise under negative voltage bias, i.e., −200 mV vs Ag/AgCl (Supporting Figure S8). The output was measured as the protonic current density, shown in Figure 6a. The results of the experiment are presented in the table shown in Table 2. We compared the output current density values under four input conditions: (0,0), (0,1), (1,0), and (1,1). The charge densities for quantifying the number of transported protons are listed in Figure 6b. A positive voltage was continuously applied across the device during the measurements to drive proton transport in the ion channel and create a PMF for ATP synthesis. The proton current was the lowest in the biosensor when 2 mM Ca^{2+} was present in the absence of ADP molecules in the solution. This can be attributed to the blocking of the gA ion channel, preventing proton transport,

Table 2. Truth Table of the gA-ATP Synthase Enzyme Logic[a]

input A		input B		output	
logic	ADP	logic	Ca^{2+}	current density	logic
0	0 mM	0	0 mM	2.5 μA cm^{-2}	0
0	0 mM	1	10 mM	0 μA cm^{-2}	1
1	2 mM	0	0 mM	4.5 μA cm^{-2}	1
1	2 mM	1	10 mM	0.7 μA cm^{-2}	0

[a]Input A, input B, and output are ADP, Ca^{2+}, and current density, respectively.

while ATP synthase remains inactive. Under other conditions, particularly in the absence of Ca^{2+} and presence of ADP molecules, the proton current showed the highest values because the ion channel was unblocked and ATP synthase was activated. Conversely, in the presence of Ca^{2+} and in the absence of ADP molecules, the proton current showed the lowest values because the ion channel was blocked by Ca^{2+} and ATP synthase was inactive. We considered these conditions as output = 1, corresponding to inputs (0,1) and (1,0) (Supporting Figure S9). Thus, we successfully integrated our proton biotransducer with a biological system in which the output signal was activated by two chemical input signals: Ca^{2+} and ADP. These inputs effectively controlled proton transport via the gA ion channel and ATP synthase. Through this expansion of our research, we have substantiated the establishment of a foundational AND logic gate using ATP synthase, as detailed in Supporting Figures S10 and Table S2. Furthermore, we have elucidated that the employment of gramicidin A (gA) in isolation does not constitute a viable logic system, as evidenced in Supporting Figure S11 and Table S3. The integration of gA with ATP synthase, forming a complex XOR gate, underscores the critical role of this combination in refined ion transport control. This significant insight highlights the hybrid system's capacity to enable complex biological computations, a promising feature for the future development of advanced bioelectronic devices.

4. CONCLUSIONS

We used a combination of an SPA proton biotransducer and SLBs to precisely regulate the proton signal within the hybrid system of the gA channel and ATP synthase through an applied voltage. The microelectrodes were fabricated using photolithography, and the SPA film was coated via electro-

https://doi.org/10.1021/acsami.3c15251
ACS Appl. Mater. Interfaces 2024, 16, 7480−7488

polymerization. The AC impedance was measured using EIS, allowing us to determine the structures of the SPA electrode, SPA-SLBs, and SPA-SLBs/gA circuits. To control the proton transport in the gA channel, we measured the current density induced by the applied voltage. We also introduced inhibitors and removers to control the proton transport. In addition, the ion current in the gA and ATP synthase hybrid systems was separately modulated by applying specific voltages and using different chemicals. To demonstrate the versatility of the proposed biodevice, we integrated it into a logic gate. By manipulating the two chemical inputs, we successfully controlled the output current density, demonstrating the functionality of the XOR logic gate. The biotransducer has significant potential for controlling ion transport beyond protons. It can be integrated with other ion channels or biological systems and combined with bioelectrical circuits to serve as a logic gate. These findings pave the way for further advancements by providing a foundation for utilizing gA-ATP synthase hybrid system as a functional component in iontronic logic-based applications.

■ ASSOCIATED CONTENT

Supporting Information

The Supporting Information is available free of charge at https://pubs.acs.org/doi/10.1021/acsami.3c15251.

Fabrication process; impedance spectra of gA-SLBs; current signal for gA-SLBs, Alamethicin-SLB, and gA-ATP synthase-SLBs in biotransducer; charge density of gA-SLBs, ATP synthase-SLBs, and gA-ATP synthase-SLBs in biotransducer; impedance fitting parameters; true table of ATP synthase; and gA enzyme logic (PDF)

■ AUTHOR INFORMATION

Corresponding Author

Takeo Miyake − *Graduate School of Information, Production and Systems, Waseda University, Kitakyushu 808-0135 Fukuoka, Japan; PRESTO, Japan Science and Technology Agency, Kawaguchi 332-0012 Saitama, Japan;* orcid.org/0000-0002-7445-633X; Email: miyake@waseda.jp

Authors

Yukun Chen − *Graduate School of Information, Production and Systems, Waseda University, Kitakyushu 808-0135 Fukuoka, Japan*

Gábor Méhes − *Graduate School of Information, Production and Systems, Waseda University, Kitakyushu 808-0135 Fukuoka, Japan;* orcid.org/0000-0003-4859-1359

Bingfu Liu − *Graduate School of Information, Production and Systems, Waseda University, Kitakyushu 808-0135 Fukuoka, Japan*

Liyun Gao − *Graduate School of Information, Production and Systems, Waseda University, Kitakyushu 808-0135 Fukuoka, Japan*

Mingyin Cui − *Graduate School of Information, Production and Systems, Waseda University, Kitakyushu 808-0135 Fukuoka, Japan*

Chenliang Lin − *Graduate School of Information, Production and Systems, Waseda University, Kitakyushu 808-0135 Fukuoka, Japan*

Yoko Hirono-Hara − *Department of Environmental and Life Sciences, School of Food and Nutritional Sciences, University of Shizuoka, Shizuoka 422-8526, Japan*

Kiyotaka Y. Hara − *Department of Environmental and Life Sciences, School of Food and Nutritional Sciences, University of Shizuoka, Shizuoka 422-8526, Japan*

Noriyo Mitome − *Faculty of Education, Tokoha University, Shizuoka 422-8581, Shizuoka, Japan*

Complete contact information is available at: https://pubs.acs.org/10.1021/acsami.3c15251

Author Contributions

T.M. conceived the study. T.M. and N.M. designed the experiments. Y.C., B.L., L.G., M.C., and N.M. performed the experiments. Y.C. and T.M. analyzed the data. Y.C., Y.H.H., K.Y.H., and N.M. prepared the ATP synthase. Y.C., G.M., and T.M. wrote the manuscript.

Notes

The authors declare no competing financial interest.

■ ACKNOWLEDGMENTS

This study was supported by JST and PRESTO (Grant Number: JPMJPR20B8). A portion of this work was conducted at the Kitakyushu Foundation for the Advancement of Industry, Science, and Technology, Semiconductor Center, and supported by the Nanotechnology Platform Program of the Ministry of Education, Culture, Sports, Science, and Technology, Japan. Noriyo Mitome was supported by the Cooperative Research Program of the NJRC Mater. & Dev. The authors thank Dr. Toshiharu Suzuki and Dr. Masasuke Yoshida for providing the expression plasmid for ATP synthase. Received: ((will be filled in by the editorial staff)) Revised: ((will be filled in by the editorial staff)) Published online: ((will be filled in by the editorial staff))

■ REFERENCES

(1) Yin, S.; Jin, Z.; Miyake, T. Wearable High-Powered Biofuel Cells Using Enzyme/Carbon Nanotube Composite Fibers on Textile Cloth. *Biosens. Bioelectron.* **2019**, *141*, No. 111471.

(2) Yin, S.; Liu, X.; Kobayashi, Y.; Nishina, Y.; Nakagawa, R.; Yanai, R.; Kimura, K.; Miyake, T. A Needle-Type Biofuel Cell Using Enzyme/Mediator/Carbon Nanotube Composite Fibers for Wearable Electronics. *Biosens. Bioelectron.* **2020**, *165*, No. 112287.

(3) Yin, S.; Liu, X.; Kaji, T.; Nishina, Y.; Miyake, T. Fiber-Crafted Biofuel Cell Bracelet for Wearable Electronics. *Biosens. Bioelectron.* **2021**, *179*, No. 113107.

(4) Takamatsu, T.; Sijie, Y.; Shujie, F.; Xiaohan, L.; Miyake, T. Multifunctional High-Power Sources for Smart Contact Lenses. *Adv. Funct. Mater.* **2020**, *30* (29), No. 1906225.

(5) Méhes, G.; Roy, A.; Strakosas, X.; Berggren, M.; Stavrinidou, E.; Simon, D. T. Organic Microbial Electrochemical Transistor Monitoring Extracellular Electron Transfer. *Adv. Sci.* **2020**, *7* (15), No. 2000641.

(6) Paulsen, B. D.; Tybrandt, K.; Stavrinidou, E.; Rivnay, J. Organic Mixed Ionic−Electronic Conductors. *Nat. Mater.* **2020**, *19* (1), 13−26.

(7) Kost, J.; Horbett, T. A.; Ratner, B. D.; Singh, M. Glucose-Sensitive Membranes Containing Glucose Oxidase: Activity, Swelling, and Permeability Studies. *J. Biomed. Mater. Res.* **1985**, *19* (9), 1117−1133.

(8) Albin, G.; Horbett, T. A.; Ratner, B. D. Glucose Sensitive Membranes for Controlled Delivery of Insulin: Insulin Transport Studies. *J. Controlled Release* **1985**, *2*, 153−164.

(9) Kageyama, I.; Kato, R.; Sawada, K.; Hattori, T. Evaluation of Acetylcholine Release and Hold Electrochemical Device by CCD Type Ion Image Sensor. *ECS Trans.* **2016**, *75* (16), 209.

(10) Miyake, T.; Josberger, E. E.; Keene, S.; Deng, Y.; Rolandi, M. An Enzyme Logic Bioprotonic Transducer. *APL Mater.* **2015**, *3* (1), No. 014906.
(11) Méhes, G.; Vagin, M.; Mulla, M. Y.; Granberg, H.; Che, C.; Beni, V.; Crispin, X.; Berggren, M.; Stavrinidou, E.; Simon, D. T. Solar Heat-Enhanced Energy Conversion in Devices Based on Photosynthetic Membranes and PEDOT:PSS-Nanocellulose Electrodes. *Adv. Sustainable Syst.* **2020**, *4* (1), No. 1900100.
(12) Cui, M.; Takahashi, M.; Chen, Y.; Liu, B.; Ohta, Y.; Miyake, T. pH Modulation in Adhesive Cells with a Protonic Biotransducer. *Bioelectrochemistry* **2022**, *147*, No. 108202.
(13) Strakosas, X.; Selberg, J.; Hemmatian, Z.; Rolandi, M. Taking Electrons out of Bioelectronics: From Bioprotonic Transistors to Ion Channels. *Adv. Sci.* **2017**, *4* (7), No. 1600527.
(14) Seitanidou, M.; Tybrandt, K.; Berggren, M.; T Simon, D. Overcoming Transport Limitations in Miniaturized Electrophoretic Delivery Devices. *Lab Chip* **2019**, *19* (8), 1427−1435.
(15) Luo, L.; Manda, S.; Park, Y.; Demir, B.; Sanchez, J.; Anantram, M. P.; Oren, E. E.; Gopinath, A.; Rolandi, M. DNA Nanopores as Artificial Membrane Channels for Bioprotonics. *Nat. Commun.* **2023**, *14* (1), No. 5364.
(16) Hemmatian, Z.; Keene, S.; Josberger, E.; Miyake, T.; Arboleda, C.; Soto-Rodríguez, J.; Baneyx, F.; Rolandi, M. Electronic Control of H+ Current in a Bioprotonic Device with Gramicidin A and Alamethicin. *Nat. Commun.* **2016**, *7* (1), No. 12981.
(17) Watanabe, R. Microsystem for the Single Molecule Analysis of Membrane Transport Proteins. *Biochim. Biophys. Acta, Gen. Subj.* **2020**, *1864* (2), No. 129330, DOI: 10.1016/j.bbagen.2019.03.016.
(18) Hemmatian, Z.; Tunuguntla, R. H.; Noy, A.; Rolandi, M. Electronic Control of H+ Current in a Bioprotonic Device with Carbon Nanotube Porins. *PLoS One* **2019**, *14* (2), No. e0212197.
(19) Misra, N.; Martinez, J. A.; Huang, S.-C. J.; Wang, Y.; Stroeve, P.; Grigoropoulos, C. P.; Noy, A. Bioelectronic Silicon Nanowire Devices Using Functional Membrane Proteins. *Proc. Natl. Acad. Sci. U.S.A.* **2009**, *106* (33), 13780−13784.
(20) Tunuguntla, R. H.; Bangar, M. A.; Kim, K.; Stroeve, P.; Grigoropoulos, C.; Ajo-Franklin, C. M.; Noy, A. Bioelectronic Light-Gated Transistors with Biologically Tunable Performance. *Adv. Mater.* **2015**, *27* (5), 831−836.
(21) Huang, S.-C. J.; Artyukhin, A. B.; Misra, N.; Martinez, J. A.; Stroeve, P. A.; Grigoropoulos, C. P.; Ju, J.-W. W.; Noy, A. Carbon Nanotube Transistor Controlled by a Biological Ion Pump Gate. *Nano Lett.* **2010**, *10* (5), 1812−1816.
(22) Chen, Y.; Cui, M.; Lin, C.; Liu, B.; Mitome, N.; Miyake, T. Enzymatic Bioluminescence Modulation with an ATP Synthase Integrated Biotransducer. *Adv. Mater. Technol.* **2022**, *7* (1), No. 2100729, DOI: 10.1002/admt.202100729.
(23) Katz, E.; Privman, V. Enzyme -Based Logic Systems for Information Processing. *Chem. Soc. Rev.* **2010**, *39* (5), 1835−1857.
(24) Poghossian, A.; Katz, E.; Schöning, M. J. Enzyme Logic AND-Reset and OR-Reset Gates Based on a Field-Effect Electronic Transducer Modified with Multi-Enzyme Membrane. *Chem. Commun.* **2015**, *51* (30), 6564−6567.
(25) Poghossian, A.; Malzahn, K.; Abouzar, M. H.; Mehndiratta, P.; Katz, E.; Schöning, M. J. Integration of Biomolecular Logic Gates with Field-Effect Transducers. *Electrochim. Acta* **2011**, *56* (26), 9661−9665.
(26) Molinnus, D.; Poghossian, A.; Keusgen, M.; Katz, E.; Schöning, M. J. Coupling of Biomolecular Logic Gates with Electronic Transducers: From Single Enzyme Logic Gates to Sense/Act/Treat Chips. *Electroanalysis* **2017**, *29* (8), 1840−1849.
(27) Zhang, Z.; Kashiwagi, H.; Kimura, S.; Kong, S.; Ohta, Y.; Miyake, T. A Protonic Biotransducer Controlling Mitochondrial ATP Synthesis. *Sci. Rep.* **2018**, *8* (1), No. 10423.
(28) Gribkova, O. L.; Nekrasov, A. A.; Ivanov, V. F.; Zolotorevsky, V. I.; Vannikov, A. V. Templating Effect of Polymeric Sulfonic Acids on Electropolymerization of Aniline. *Electrochim. Acta* **2014**, *122*, 150−158.
(29) Belgherbi, O.; Seid, L.; Lakhdari, D.; Chouder, D.; Akhtar, M. S.; Saeed, M. A. Optical and Morphological Properties of Electropolymerized Semiconductor Polyaniline Thin Films: Effect of Thickness. *J. Electron. Mater.* **2021**, *50* (7), 3876−3884.
(30) Mitome, N.; Kubo, S.; Ohta, S.; Takashima, H.; Shigefuji, Y.; Niina, T.; Takada, S. Cooperation among C-Subunits of FoF1-ATP Synthase in Rotation-Coupled Proton Translocation. *eLife* **2022**, *11*, No. e69096.
(31) Steinem, C.; Janshoff, A.; Galla, H.-J.; Sieber, M. Impedance Analysis of Ion Transport through Gramicidin Channels Incorporated in Solid Supported Lipid Bilayers. *Bioelectrochem. Bioenerg.* **1997**, *42* (2), 213−220.
(32) Ben Tahar, A.; Zebda, A.; Alcaraz, J.-P.; Gayet, L.; Boualam, A.; Cinquin, P.; Martin, D. K. A PANI Supported Lipid Bilayer That Contains NhaA Transporter Proteins Provides a Basis for a Biomimetic Biocapacitor. *Chem. Commun.* **2019**, *55* (87), 13152−13155.
(33) Vallejo, A. E.; Gervasi, C. A. Impedance Analysis of Ion Transport through Gramicidin Channels in Supported Lipid Bilayers. *Bioelectrochemistry* **2002**, *57* (1), 1−7.
(34) Heitz, F.; Gavach, C. Ca2+-Gramicidin a Interactions and Blocking Effects on the Ionic Channel. *Biophys. Chem.* **1983**, *18* (2), 153−163.
(35) Lundbæk, J. A.; Maer, A. M.; Andersen, O. S. Lipid Bilayer Electrostatic Energy, Curvature Stress, and Assembly of Gramicidin Channels. *Biochemistry* **1997**, *36* (19), 5695−5701.
(36) Yue, J.; Epstein, A. J. Electronic Control of pH at Sulfonated Polyaniline Electrodes. *J. Chem. Soc., Chem. Commun.* **1992**, *1* (21), 1540−1542, DOI: 10.1039/C39920001540.